BIOCHEMICAL PHARMACOLOGY 72 (2006) 597–607

available at www.sciencedirect.com

ScienceDirect

journal homepage: www.elsevier.com/locate/biochempharm

Crystal structures of acetylcholinesterase in complex with HI-6, Ortho-7 and obidoxime: Structural basis for differences in the ability to reactivate tabun conjugates☆,☆☆

Fredrik Ekström [a,*], *Yuan-Ping Pang* [b], *Malin Boman* [a], *Elisabet Artursson* [a], *Christine Akfur* [a], *Susanne Börjegren* [a]

[a] *Swedish Defense Research Agency, Division of NBC Defense, S-901 82, Umeå, Sweden*
[b] *Computer-Aided Molecular Design Laboratory, Mayo Clinic College of Medicine, 200 First Street SW, Rochester, MN, 55905, USA*

ARTICLE INFO

Article history:
Received 20 April 2006
Accepted 24 May 2006

Keywords:
Acetylcholinesterase
HI-6
Ortho-7
Obidoxime
X-ray crystallography
Structural change

Abbreviations:
ACh, acetylcholine
AChE, acetylcholinesterase
eAChE, *Electrophorus electricus* acetylcholinesterase
DTNB, 5,5′-dithiobis(2-nitrobenzoic acid)
DFP, diisopropyl phosphorofluoridate
Echothiophate, *O*,*O*′-diethyl S-2-trimethylaminoethyl phosphorothiolate iodide

ABSTRACT

Inhibition of acetylcholinesterase (AChE) by organophosphorus compounds (OPs) such as pesticides and nerve agents causes acute toxicity or death of the intoxicated individual. The inhibited AChE may be reactivated by certain oximes as antidotes for clinical treatment of OP-intoxications. Crystal structures of the oximes HI-6, Ortho-7 and obidoxime in complex with *Mus musculus* acetylcholinesterase (mAChE) reveal different roles of the peripheral anionic site (PAS) in the binding of the oximes. A limited structural change of the side chains of Trp286 and Asp74 facilitates the intercalation of the 4-carboxylamide pyridinium ring of HI-6 between the side chains of Tyr124 and Trp286. The 2-carboxyimino pyridinium ring of HI-6 is accommodated at the entrance of the catalytic site with the oximate forming a hydrogen bond to the main-chain nitrogen atom of Phe295. In contrast to HI-6, the coordination of Ortho-7 and obidoxime within the PAS is facilitated by an extended structural change of Trp286 that allows one of the carboxyimino pyridinium rings to form a cation-π interaction with the aromatic groups of Tyr72 and Trp286. The central chain of Ortho-7 and obidoxime is loosely coordinated in the active-site gorge, whereas the second carboxyimino pyridinium ring is accommodated in the vicinity of the phenol ring of Tyr337. The structural data clearly show analogous coordination of Ortho-7 and obidoxime within the active-site gorge of AChE. Different ability to reactivate AChE inhibited by tabun is shown in end-point reactivation experiments where HI-6, Ortho-7 and obidoxime showed an efficiency of 1, 45 and 38%, respectively. The low efficiency of HI-6 and the significantly higher efficiency of Ortho-7 and obidoxime may be explained by the differential binding of the oximes in the PAS and active-site gorge of AChE.

☆ Protein Data Bank entry codes are 2GYU, 2GYV and 2GYW for the structures of mAChE·HI-6, mAChE·Ortho-7 and mAChE·obidoxime, respectively.

☆☆ This work was supported by the Swedish Armed Forces Research and Technology Program. Yuan-Ping Pang was supported by the Defense Advanced Research Projects Agency of USA (DAAD19-01-1-0322).

* *Corresponding author*. Tel.: +46 90 106815; fax: +46 90 106800.
E-mail address: fredrik.ekstrom@foi.se (F. Ekström).

0006-2952/$ – see front matter
doi:10.1016/j.bcp.2006.05.027

HI-6, 1-(2-hydroxy-iminomethylpyridinium)-1-(4-carboxyamino)-pyridinium dimethylether dichloride
hAChE
Homo sapiens acetylcholinesterase
HLö-7, 1-[[[4-(aminocarbonyl) pyridinio]methoxy]metyl]-2,4-bis [(hydroxyimino)methyl] pyridinium dimethanedisulfonate
mAChE, *Mus musculus* acetylcholinesterase
MEPQ, 7-(*O*-ethyl methylphosphinyloxy)-1-methylquinolinium iodide
Obidoxime, 1,1′-(oxydimethylene) bis(4-formylpyridinium) dioxime
OP, organophosphorus compound
Sarin, methylethyl methylphosphonofluoridate
Ortho-7, 1,7-heptylene-bis-*N*,*N*′-2-pyridiniumaldoxime dichloride
Paraoxon, diethyl *p*-nitrophenyl phosphate
Soman, 1,2,2-trimethylpropyl methylphosphonofluoridate
PAS, peripheral anionic site
Tabun, ethyl *N*,*N*-dimethylphosphoramidocyanidate
TMB-4, 1,1′-trimethylenebis (4-formylpyridinium bromide) dioxime
TcAChE, *Torpedo californica* acetylcholinesterase
TMTFA, *m*-(*N*,*N*,*N*-trimethylammonio)-2,2,2-trifluoroacetophenone
VX, *O*-ethyl S-2-isopropylaminoethyl methylphosphonothiolate
2-PAM, 2-pyridine aldoxime

1. Introduction

Acetylcholinesterase (AChE) terminates cholinergic neurotransmission by catalyzing the hydrolysis of the neurotransmitter acetylcholine (ACh). The catalytic triad consists of Ser203, Glu334 and His447, residues located close to the base of a deep active-site gorge that penetrates about 20 Å into the enzyme [1]. The lining of the active-site gorge is mostly assembled by aromatic side chains that form a narrow entrance to the catalytic Ser203. At the surface of the protein, a peripheral anionic site (PAS) is located at the rim of the active-site gorge where it provides a binding site for allosteric modulators and PAS inhibitors [2–4]. As recognized today, PAS comprises aromatic residues Tyr72, Tyr124, Trp286 and Tyr341 and acidic residue Asp74 [2].

Acetylcholinesterase is susceptible to irreversible inhibition by organophosphorus compounds (OPs), a class of inhibitors that includes organophosphorus pesticides and nerve agents. Organophosphorus compounds inhibit AChE by forming a phosphorus conjugate that is covalently attached to the catalytic serine residue. In some cases, the phosphorous conjugate can affect the conformation of the distantly located PAS [5]. The function of the inhibited enzyme may be restored by a reaction with nucleophilic reactivators, a process known as reactivation, exemplified in Scheme 1. Therapeutic reactivators such as 2-PAM, obidoxime and HI-6 share an oxime functionality that is attached to a pyridinium ring to facilitate a nucleophilic attack on the AChE–OP conjugate. The efficiency of these molecules depends on the chemical nature of the OP conjugate, the source and sequence of the enzyme as well as the chemical structure of the oxime [6,7].

The molecular scaffold of early oximes such as 2-PAM contained a single pyridinium ring [8]. By connecting two pyridinium rings with a central linker, the potency of oximes was improved [9–11]. In a recent effort to further improve the efficiency of oximes, the symmetrical bis-pyridiniumaldoxime Ortho-7 was generated [12]. Studies of Ortho-7-mediated reactivation of AChE inhibited by isofluorophate show that Ortho-7 was effective both *in vitro* and *in vivo* for this particular OP compound [12,13]. However, the potency of Ortho-7 on

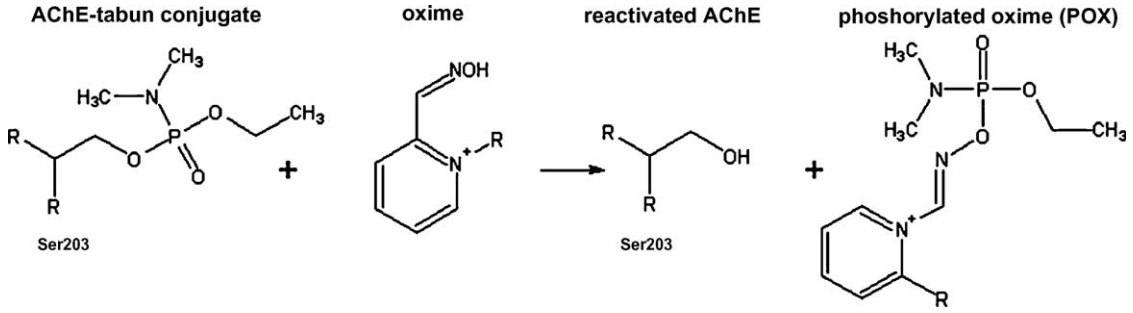

Scheme 1 – Scheme describing the reactivation of tabun inhibited AChE.

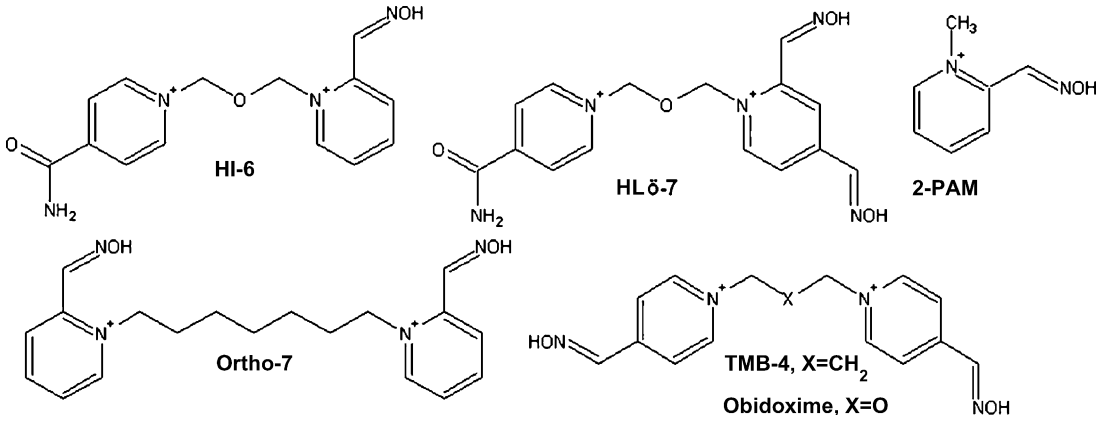

Fig. 1 – Chemical structures of reactivators.

certain AChE–OP conjugates that are highly resistant towards reactivation (e.g., conjugates of tabun) is not known. Modelling studies have suggested that one of the pyridinium rings of Ortho-7 interacts with the PAS of AChE, whereas the second pyridinium ring is accommodated in the vicinity of the choline binding site [12].

Reactivation kinetics of site-directed substitutions show that PAS is important for reactivation by HI-6 on various phosphorous conjugates [14–16]. Inhibition kinetics, reactivation kinetics and modelling studies of TMB-4 also show the involvement of PAS in the reactivation by TMB-4. Because obidoxime is structurally nearly identical to TMB-4 (Fig. 1), PAS is most likely involved in the reactivation by obidoxime as well. However, the structural details of how HI-6 and obidoxime interact with PAS are unknown. Such details are difficult to extrapolate from the modelling studies of Ortho-7 and TMB-4 since HI-6 and obidoxime are linked with ethers whereas Ortho-7 and TMB-4 are tethered with alkylenes (Fig. 1).

In this study, we present the crystal structures of HI-6, Ortho-7 and obidoxime in complex with non-phosphorylated *Mus musculus* acetylcholinesterase (mAChE).[1] We also demonstrate effective reactivation by Ortho-7 and obidoxime and poor reactivation by HI-6 for tabun-inhibited AChE. With the present findings we provide the atomic details on how HI-6 interacts with the PAS, and we suggest a hypothesis that explains why obidoxime shows reactivation of the tabun inhibited AChE similar to that of Ortho-7 and much greater than that of HI-6 despite that obidoxime and HI-6 share a similar molecular scaffold.

2. Materials and methods

2.1. Chemicals and reagents

Obidoxime (>98%) was a kind gift of Dr. Worek (Bundeswehr Institute of Pharmacology and Toxicology, Germany), HI-6 (>98%) was a gift from Dr. Clement (Defence Research Establishment, Canada) whereas Ortho-7 was synthesized as previously described [12]. Tabun was synthesized, verified by NMR and purified to a purity that exceeded 95% [17]. Acetylthiocholine iodide (>99%), DTNB (>98%), HEPES (>99.5%) and Triton X100 (laboratory grade) was purchased by Sigma Aldrich. Sodiumdihydrogenphosphate (>99%) and di-sodiumhydrogenphosphate (>99%) was obtained by Merck whereas Fluka supplied the polyethylene glycol monomethylether 750 used during the crystallization attempts.

2.2. Cloning, expression and enzymatic assays

Recombinant AChE from *Mus musculus*, used for the crystallographic studies was cloned, expressed and purified as previously reported [18]. Hydrolysis of acetylthiocholine iodide (ATC) was monitored with a modified spectrophotometric Ellman assay [19]. The assay mixture (1 mL) contained

[1] The sequence numbering of mAChE is used throughout this paper when amino acids of any AChE are discussed.

0.20 mM DTNB, 100 mM sodium phosphate pH 7.4, 0.1% Triton X100 and 1 mM ATC. All assays were performed at 30 °C.

2.3. Reactivation of AChE inhibited by tabun

Purified wild-type, *Mus musculus* AChE was inhibited with an excess of a racemic tabun solution. Complete inhibition was verified by measurements of residual enzyme activity. Excess of tabun were removed by a two consecutive buffer exchanges on NAP-5 columns (GE-healthcare), equilibrated in E-buffer composed of 100 mM sodium phosphate pH 7.4, 0.1% Triton X100. The samples were immediately incubated with 1 mM of HI-6, Ortho-7 or obidoxime at a temperature of 30 °C. A control with active (non-inhibited) AChE was subjected to the same procedure. After 15, 30, 45 and 60 min of incubation, the samples were diluted at least 2000 times in E-buffer and the restored enzyme activity, v_{ir}, was determined. The efficiency of reactivation was determined after 60 min using the equation:

$$E = 100\frac{v_{ir}\frac{v}{v_r} - v_i}{v - v_i} \quad (1)$$

where E is the percentage of the reactivated enzyme, v the control enzyme activity, v_i the residual enzyme activity in the inhibited sample, and v_r is the enzyme activity of the control sample in the presence of a reactivator.

2.4. Crystal screening and generation of AChE–oxime complexes

Crystal screening experiments were performed as previously described [18]. Binary complexes between AChE and TMB-4, obidoxime, HI-6 or Ortho-7 were generated by crystal soaking methods. Crystals were slowly allowed to equilibrate in X-buffer composed of 28% (v/v) polyethylene glycol monomethylether 750, 100 mM HEPES pH 7.0. Several hours prior to data collection, 100 μL X-buffer was saturated with solid oxime. This solution was subsequently added to the equilibrated crystals in several (~10) portions of 0.5 μL during a period of 1–2 h. The soaked crystals were further incubated in the presence of the oxime for at least 2 h prior to flash freezing in liquid nitrogen.

2.5. Collection, processing and refinement of diffraction data

Crystals were flash-frozen in liquid nitrogen and X-ray diffraction data were collected at 100 K at the MAXlab synchrotron (Lund, Sweden), beamline I711 and I911-5 on a MAR Research CCD detector. Images were collected with an oscillation angle of 1.0° per exposure and the total oscillation range covered at least 150° per data set. Intensity data were indexed and integrated with XDS [20] and scaled using Scala [21]. The structure was solved using rigid body refinement with the apo structure of mAChE as a starting model [4]. Further crystallographic refinement was carried out using restrained isotropic B-factor refinement as implemented in the program Refmac5 [22]. Refinement included 98% of the data whereas the remaining 2% was randomly excluded and used to follow the progress of the refinement with *R-free* [23]. Several rounds of refinement were performed, alternating with manual rebuilding of the model after visualization of $2|F_o| - |F_c|$ and $|F_o| - |F_c|$ maps using the program O [24]. For the final refinement rounds, TLS refinement was employed with each protein chain defined as a TLS group. The quality of the final model was evaluated using PROCHECK and WHATCHECK [25,26].

3. Results

3.1. General description and quality of the final models

The general features of the binary AChE oxime complexes are very similar to the apo structure of mAChE with minor structural distortions in the vicinity of the oxime binding sites (discussed in detail below). The asymmetric unit contains two molecules (A and B) of which the A monomer is generally

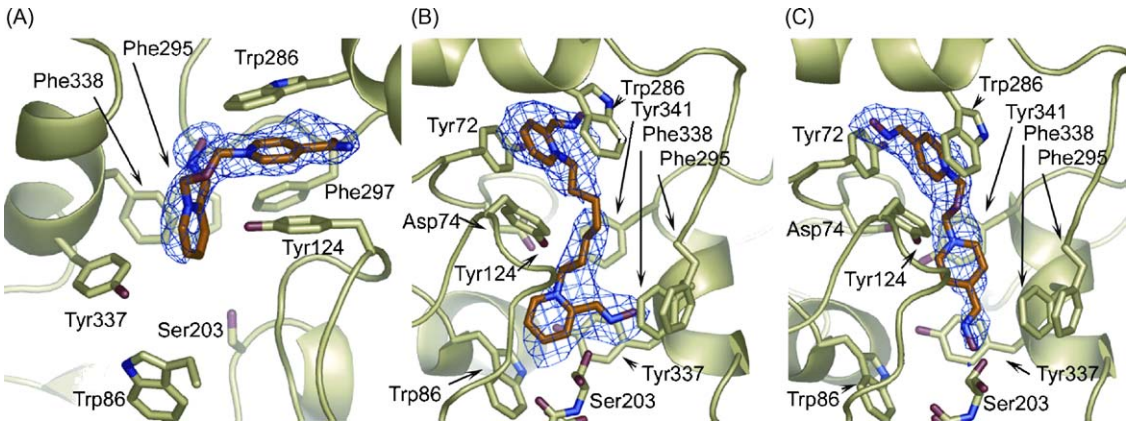

Fig. 2 – Overview of the electron density and binding of HI-6 (A) and Ortho-7 (B) and obidoxime (C) in mAChE with the $|F_o| - |F_c|$ omit map (blue) contoured at a level 3.5, 2.5 and 3.5σ, respectively. The protein carbon atoms are shown in green whereas the oxime carbon atoms are shown in orange. Nitrogen and oxygen atoms are shown in blue and red, respectively. (For interpretation of the references to color in this figure legend, the reader is referred to the web version of the article.)

better resolved in the electron density map. The loop region that consists of residues 258–264 could not be traced in the electron density. The oximes HI-6, obidoxime and Ortho-7 are easily identified as strong electron density features in the $|F_o|$-$|F_c|$ omit map (Fig. 2). The oxime binding sites are similar in the A and the B monomer of the asymmetric unit and in the following descriptions, the A monomer is considered. Attempts to identify the binding site of TMB-4 were unsuccessful, even though three independent, highly redundant data sets of TMB-4-soaked crystals were collected to a maximal resolution of 2.2 Å (data not shown). In mAChE·HI-6, mAChE·obidoxime and mAChE·Ortho-7, the electron density of Trp286 implies a small fraction of the non-complexed, apo conformation of this residue. The intermediate resolution of the present structures cause difficulties in the estimation of this low occupancy species and therefore, the apo conformation was not considered during the refinement. The significantly higher occupancy of HI-6, obidoxime and Ortho-7 was approximated to 0.8 by matching the atomic B-factors of the oximes with the B-factors of adjacent atoms. In the A monomer of the asymmetric unit, the glycosylation of residue Asp350 and Asp464 could be identified in the electron density map. The model refinement statistics is shown in Table 1. The Ramachandran plot show unusual phi and psi angle for the main-chain atoms of Ser203. The electron density clearly defines the conformation of the backbone and it seems likely that the tight steric constraint in this part of the catalytic site cause the disallowed conformation of Ser203.

3.2. *Crystal structure of mAChE in complex with HI-6*

The main feature of the 2.2 Å crystal structure of HI-6 in complex with mAChE (mAChE·HI-6) is a strong cation-π interaction between the 4-carboxylamide-pyridinium ring (designated the peripheral pyridinium ring) and the side chains of Tyr124 and Trp286 (Fig. 3). The interaction is facilitated by the movement of the side chain of Trp286 towards Asp74 that allows the carboxylamide-pyridinium to be sandwiched by the indole ring of Trp286 and the phenol ring of Tyr124. The carboxylamide moiety has a hydrogen bond (2.9 Å) between the carboxyl O3 oxygen and the main-chain nitrogen of Ser298 and a hydrogen bond (2.8 Å) between the amide N4 nitrogen and a water molecule (W260). This water molecule is further coordinated by a hydrogen bond to the side chain of Glu285. The central linker of HI-6 is directed into the active-site gorge where the side chain of Asp74 assumes a previously not observed conformation that allows a hydrogen bond (3.0 Å) to the ether O2 oxygen of the HI-6 linker. The atomic B-factors of the side chain of Asp74 are relatively high and the electron density of Asp74 is weak, features symptomatic with a mobility of the Asp74 side chain. The 2-hydroxy-iminomethylpyridinium ring is directed towards the catalytic site, and it is stabilized by non-bonded contacts to the side chains of Tyr337, Phe338 and Tyr341 including a weak (3.3 Å) hydrogen bond between the N2 nitrogen and the phenol group of Tyr124. The torsion of the attacking oximate (O1–N1–C1–C2) is approximately 60° of arc, and this unusual torsion value is probably due to a 2.9 Å

Table 1 –

Data collection	mAChE·HI-6	mAChE·Ortho-7	mAChE·obidoxime
Space group	$P2_12_12_1$	$P2_12_12_1$	$P2_12_12_1$
Unit cell dimensions (Å)	78.16 × 110.72 × 226.25	76.73 × 108.58 × 220.58	79.06 × 111.53 × 227.36
Resolution range (Å)	28.95–2.20 (2.32–2.20)	29.0–2.50 (2.64–2.50)	29.67–2.40 (2.53–2.40)
Total number of reflections	713462 (102321)	478819(69692)	589021 (85515)
Unique reflections	100429 (14491)	64151 (9236)	79454(11478)
Completeness (%)	100.0 (100.0)	99.4(99.1)	99.9 (100.0)
Multiplicity	7.1(7.1)	7.5 (7.5)	7.4 (7.5)
R_{Merge}[a]	0.069(0.519)	0.086 (0.507)	0.088 (0.554)
Mean (I)/S.D. (I)	19.6 (4.7)	19.6 (4.8)	16.8 (4.4)
Refinement			
R-factor/R_{free} (%)[b,c]	19.7/22.5	19.7/24.1	19.6/23.2
B-factor (Å)[d]	43.0/43.0	40.4/40.8	43.2/43.2
Number of water molecules	518	343	368
RMS from ideal values			
Bond lengths (Å)	0.011	0.014	0.012
Bond angle (°)	1.468	1.545	1.444
Ramachandran plot (%)/no. of residues			
Most favoured regions	91.0/802	88.9/783	89.0/784
Additional allowed regions	8.4/74	10.3/94	10.6/93
Generously allowed regions	0.5/4	0.3/3	0.2/2
Residues in disallowed regions	0.1/1[e]	0.1/1[e]	0.2/2[e]

[a] $R_{merge} = (\sum|I - \langle I\rangle|)/\sum I$, where I is the observed intensity and $\langle I\rangle$ is the average intensity obtained after multiple observations of symmetry related reflections.
[b] R-factor = $(\sum||F_o| - |F_c||)/\sum F_o$, where F_o are observed and F_c are calculated structure factors.
[c] R_{free} uses 2% randomly chosen reflections defined in Brunger [23].
[d] B-factor is the mean factor for protein main-chain A/B.
[e] The residue located in the disallowed regions is Ser203 (see also Section 3).

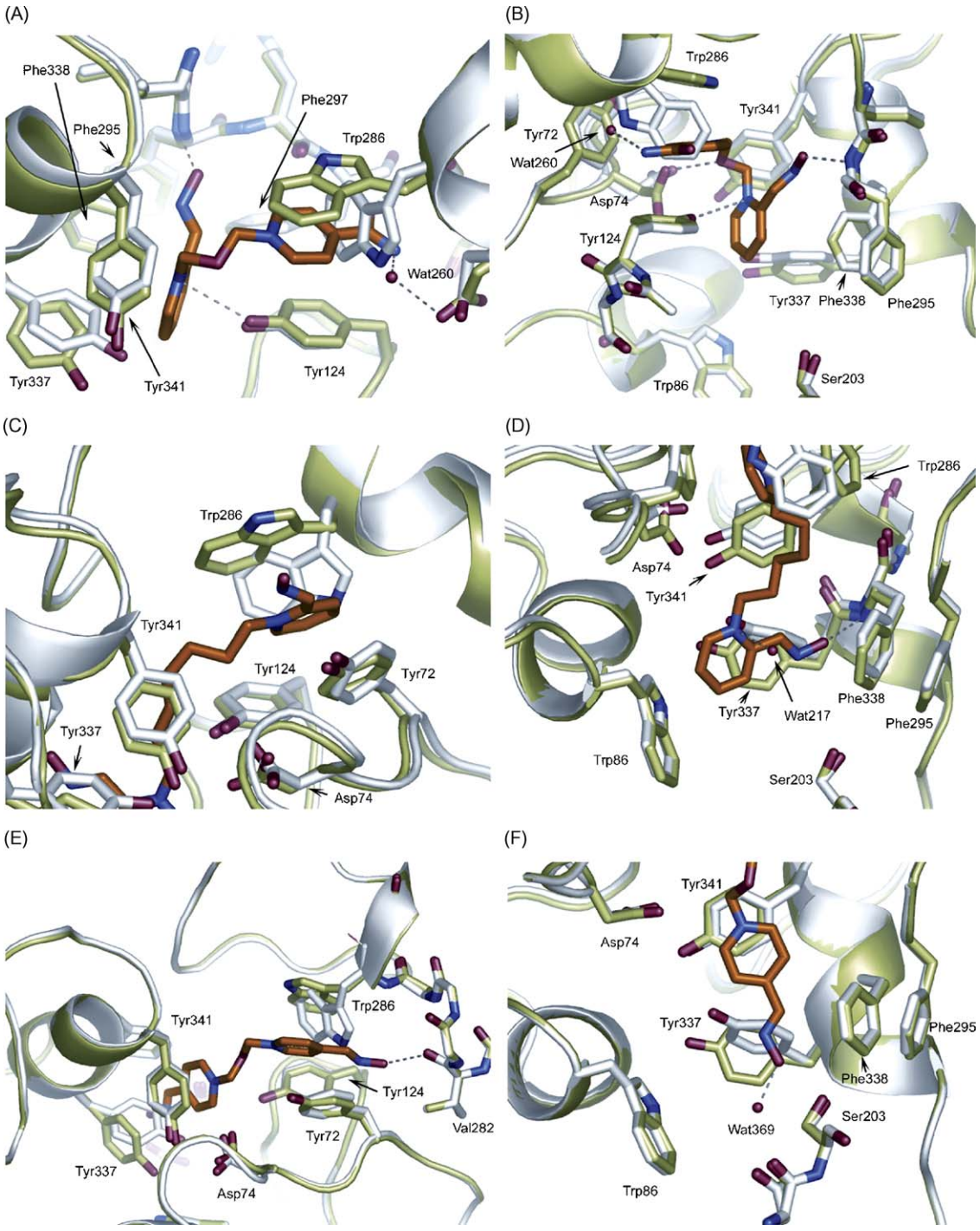

Fig. 3 – The interaction between the PAS of mAChE and HI-6 (A), Ortho-7 (C) and obidoxime (E) and the corresponding interaction with the catalytic site shown for HI-6 (B), Ortho-7 (D) and obidoxime (E). The oxime-bound structures and the apo structure (PDB entry 1J06) are shown in green and grey, respectively. Water molecules are shown as red spheres, oxygen atoms are shown in red, nitrogen atoms in blue and hydrogen bonds as dashed lines. (For interpretation of the references to color in this figure legend, the reader is referred to the web version of the article.)

hydrogen bond between the O1 oxygen of the oxime moiety and the main-chain nitrogen of Phe295. The closest distance between the HI-6 molecule and the catalytic Ser203 is 6.6 Å measured between the pyridinium C4 of HI-6 and Oγ of Ser203.

3.3. *Crystal structure of mAChE in complex with Ortho-7*

The crystal structure of mAChE in complex with Ortho-7 (mAChE·Ortho-7) was determined to a resolution of 2.5 Å (Table 1). Similar to HI-6, Ortho-7 induces a structural change

of the indol ring of Trp286 that undergoes an extended movement towards Asp74. The distortion of Trp286 allows one of the pyridinium rings (designated the peripheral pyridinium ring) of Ortho-7 to form cation-π interactions with the side chains of Tyr72 and Trp286 (Fig. 3). In contrast to HI-6, the peripheral pyridinium ring does not participate in any hydrogen bonds. The central heptyl chain of Ortho-7 is aligned in an extended conformation along the axis of the active-site gorge with non-bonded contacts, mainly to the side chains of Tyr124 and Tyr341. The electron density map of the central linker is relatively weak, implying a conformational flexibility of the heptyl chain. The second pyridinium ring of Ortho-7 has a nearly parallel cation-π interaction with the phenyl ring of Tyr337 and a T-shaped cation-π interaction with the indole ring of Trp86. Therefore, the oximate O1 oxygen is tightly sandwiched by Tyr337 and Phe338, with several close contacts (2.9–3.1 Å) including a weak hydrogen bond (3.1 Å) to the main-chain nitrogen of Phe338. A small compensatory distortion of the side chain of Tyr337 positions the aromatic ring with a close contact with the side chain of Tyr341. The pyridinium ring of Ortho-7 has a hydrogen bond (3.0 Å) to a water molecule (W217). Both oxime groups of Ortho-7 are nearly in plane with the pyridinium rings.

3.4. *Crystal structure of mAChE in complex with obidoxime*

The 2.4 Å crystal structure of mAChE in complex with obidoxime (mAChE·obidoxime) shows that the pyridinium oxime has a hydrogen bond (3.2 Å) with the carbonyl oxygen of Val282 and similar to AChE-Ortho-7, cation-π interactions with the side chains of Trp286 and Tyr72 (Table 1; Fig. 3). The central chain of obidoxime is accommodated in the active-site gorge with no hydrogen-bonding partner for the ether oxygen. The pyridinium ring that carries the attacking oxime forms cation-π interactions with the aromatic surface that is created by the side chains of Tyr337 and Tyr341. A small compensatory distortion of the side chain of Tyr337 is observed in this region of the protein. The C1 carbon of the oxime moiety is coordinated by a 3.3 Å contact with the Cε2 carbon of Phe338 whereas the oxime oxygen of obidoxime forms a close hydrogen bond to a water molecule (W368). Like Ortho-7, both oxime groups of obidoxime are in plane with the pyridinium rings.

3.5. *Reactivation of hAChE Inhibited by tabun*

Although AChE inhibited by tabun is considered very resistant towards reactivation, obidoxime is known to reactivate tabun conjugates with a moderately efficiency. The ability of HI-6, Ortho-7 and obidoxime to reactivate mAChE inhibited by tabun were compared in endpoint experiments. The enzyme was inhibited by tabun and subsequently incubated with the oxime at a concentration of 1 mM. In these experiments, after incubation for 60 min, Ortho-7 reactivated 43%, obidoxime reactivated 38%, whereas HI-6 reactivated less than 1% of the original AChE activity.

4. Discussion

The presented crystal structures of HI-6, Ortho-7 and obidoxime in complex with non-phosphorylated mAChE reveal two distinct modes of binding to mAChE. In the case of HI-6, the peripheral pyridinium ring is sandwiched via cation-π interactions with the side chains of Tyr124 and Trp286, and two hydrogen bonds. The central linker of HI-6 extends into the active-site gorge with the ether O2 oxygen forming a hydrogen bond to Asp74. This interaction may explain why a substitution of the HI-6 ether oxygen with a methylene group reduced the reactivation potency of the oxime for the fast reacting species of MEPQ-inhibited enzyme 5-fold [16]. The oxime substituted pyridinium ring form hydrogen bonds to Phe295 and Tyr124 and cation-π interactions with Tyr337, Phe338 and Tyr341. The interaction of HI-6 with the PAS is facilitated by a limited structural change of the indole ring of Trp286. The peripheral pyridinium ring of Ortho-7 and obidoxime are sandwiched via cation-π interactions

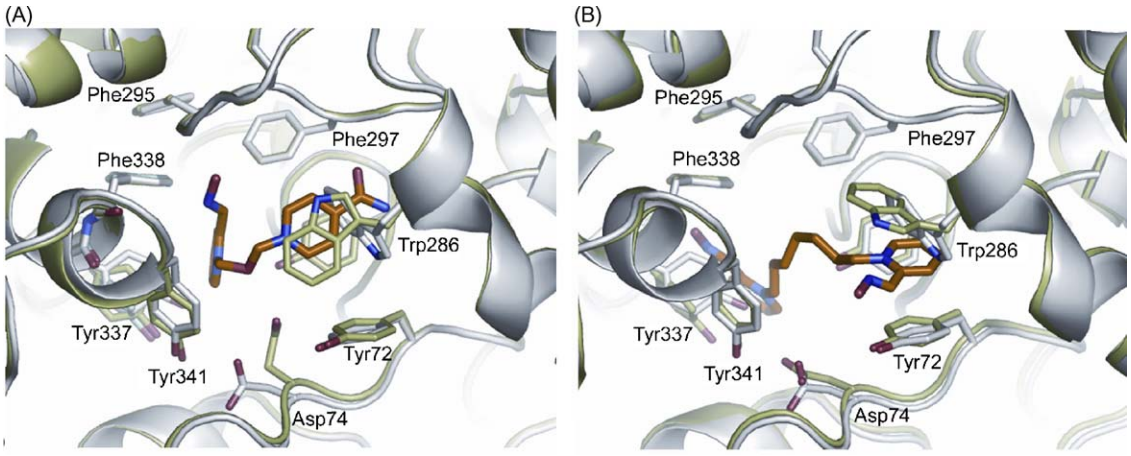

Fig. 4 – Structural alignment between mAChE·HI-6 shown in green (A), mAChE·Ortho-7 (B; green) and the apo structure of mAChE shown in grey (PDB entry 1J06). The oxime carbon atoms are shown in orange whereas the nitrogen and oxygen atoms are shown in blue and red colour, respectively. (For interpretation of the references to color in this figure legend, the reader is referred to the web version of the article.)

with the side chains of Tyr72 and Trp286. In comparison with HI-6, the PAS interaction of Ortho-7 and obidoxime requires a large conformational change of Trp286. Moreover, the peripheral pyridinium ring of Ortho-7 and obidoxime is exposed to the solvent, in contrast to the buried pyridinium ring of HI-6 (Fig. 4). In the case of Ortho-7, no hydrogen bonds participate in the PAS interaction whereas the oximate oxygen of obidoxime forms a hydrogen bond to the carbonyl oxygen of Val282. The extended displacement of the Trp286 indole side chain and the intercalation of the peripheral pyridinium ring between the aromatic rings of Trp286 and Tyr72 are rather similar to the interaction between the potent *syn*1 TZ2PA6 inhibitor and AChE [27]. The seven atom linker of Ortho-7 is loosely coordinated in the active-site gorge, and the pyridinium ring that carries the attacking oxime is located in vicinity of the choline binding site where it forms cation-π interactions with the phenol ring of Tyr337 and a T-shaped interaction with the indole ring of Trp86. In the case of obidoxime, the shorter, three atom linker positions the pyridinium ring in a slightly different position, with cation-π interactions to the aromatic surface formed by the side chains of Tyr337 and Tyr341.

A key feature of HI-6 is the 4-carboxylamide moiety of the peripheral pyridinium ring that coordinates the pyridinium ring via two hydrogen bonds. Other oximes with a 4-carboxylamide substituted pyridinium (e.g., HLö-7) are likely to interact with AChE in a corresponding fashion. In contrast, the 2-substituted pyridinium ring of Ortho-7 cannot form the equivalent hydrogen bonds and the PAS interaction of Ortho-7 relies mainly on cation-π interactions. Similar to HI-6, obidoxime has a 4-substituted peripheral pyridinium ring. However, in comparison with the carboxylamide moiety of HI-6, the geometry and size of the oxime moiety prevent obidoxime to interact with the PAS in the same way as HI-6.

Our previous modelling studies showed that TMB-4 and Ortho-7 span the active site of the phosphorylated hAChE with a distances between the two nucleophilic oxime-oxygens of 14.7 and 13.0 Å, respectively and suggested that TMB-4 and obidoxime with a 4-substituted oxime is structurally analogous to Ortho-7 with an 2-substituted oxime but not to HI-6 with an 2-substituted oxime, even though the linkers of HI-6, TMB-4 and obidoxime consist of three atoms. The structural and functional similarity between Ortho-7, TMB-4 and obidoxime and the structural dissimilarity between these oximes and HI-6 are supported by our present finding that the efficiency of reactivation of tabun-inhibited mAChE is 1, 43 and 38% for HI-6, Ortho-7 and obidoxime, respectively. It is conceivable that TMB-4 has an interaction with the PAS and the active-site gorge that is similar to the interactions described for obidoxime. This is supported by inhibition studies of Tyr72Ala and Trp286Ala substitutions that cause a more than 12-fold decrease in the affinity of TMB-4 [14]. Several attempts to determine the crystal structure of TMB-4 were unsuccessful and the reason for these difficulties is not known. In a 2.2 Å resolution data of AChE crystals soaked with TMB-4, the initial $|F_o| - |F_c|$ omit map showed a weak density feature close to Trp286; however, during subsequent model building attempts, the TMB-4 molecule could not be unambiguously identified. Based on these observations, an alternative binding site of TMB-4 cannot be excluded.

The non-phosphorylated Ser203 of mAChE·HI-6, mAChE·Ortho-7 and mAChE·obidoxime is not a substrate for reactivation, consequently, these structures may not completely represent the conformation and the chemical environment found in a phosphorylated enzyme. It has been implicated that the interaction between the phosphorous conjugate and the oxime is a central characteristics of a phosphorylated AChE–oxime complex and that the binding modes of oximes to the phosphorylated enzyme is different than the binding to a non-phosphorylated enzyme [14]. Nevertheless, our structural details described herein are useful in that our data provide an insight into the understanding of the conformational difference between the oxime-bound AChE in its phosphorylated and non-phosphorylated states. This insight leads to the following hypothesis that explains several observations made during oxime-mediated reactivations such as the effect on the reactivation rate constant for PAS substitutions and the different accommodation of HI-6 and TMB-4 within the active-site gorge of AChE [14–16].

It has been suggested that the reactivation of OP-conjugates proceeds by a trigonal bipyramidal transition state with the attacking oximate oxygen and the leaving Ser203 oxygen in apical positions [15,28]. The crystal structures of *Torpedo californica* AChE (TcAChE) inhibited by VX (TcAChE-VX) and the structure of mAChE inhibited by tabun (mAChE–tabun) are available [18,29]. It has been shown that HI-6 is an efficient reactivator of AChE inhibited by VX, whereas tabun conjugates are notably resistant towards the reactivation by HI-6 [7]. A structural alignment of mAChE·HI-6 with TcAChE-VX and mAChE–tabun suggest that a relocalization of the attacking oxime from the binding site observed in mAChE·HI-6, probably to the vicinity of the hydrophobic pocket formed by the side chains of Trp86, Tyr337 and Phe338 is necessary to enable the nucleophilic attack on the tabun conjugate (Fig. 5). A relocalization of HI-6 from the site observed in mAChE·HI-6 would most likely allow the indole ring of Trp286 to assume the apo conformation and thus, allow the phosphorylated oxime to leave the active-site gorge after the reactivation reaction. In the case of tabun conjugates, a structural change of the inhibited enzyme positions the side chain of Phe338 in the vicinity of the oxime substituted pyridinium ring of HI-6. In fact, the distance between the Cε2 atom of Phe338 in mAChE–tabun and the C2 atom of HI-6 in mAChE·HI-6 is only 1.4 Å, suggesting that the steric blockage by Phe338 could severely interfere with the entrance of HI-6 into the catalytic site of AChE–tabun conjugates [18]. Alternative attacking orientations of oximes have previously been proposed in studies of HI-6-mediated reactivation of site-directed substitutions [16,30,31]. The low efficiency of HI-6 on reactivating hAChE inhibited by tabun suggests the alternative attacking orientations of HI-6 is not compatible with tabun conjugates. The steric blockage by the side chain of Phe338 in tabun conjugates may not be relevant to the oxime HLö-7 that have an oxime moiety at the 4-position of the pyridinium ring and consequently, is be able to attack the phosphorous conjugate without experiencing the steric hindrance. This hypothesis is consistent with the report that the oxime HLö-7 is able to reactivate tabun conjugates [7,32,33].

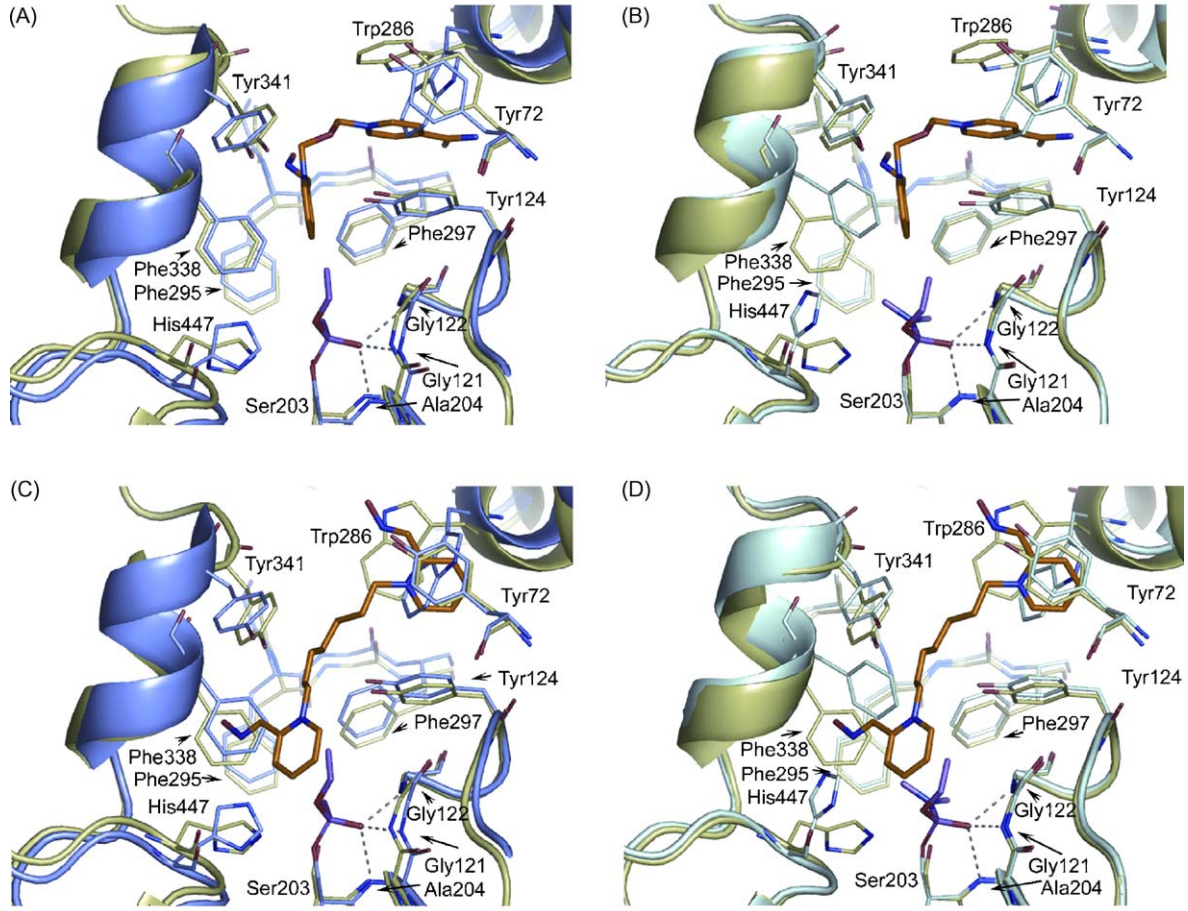

Fig. 5 – Structural alignments of TcAChE-VX (A and C; PDB entry 1VXR) and mAChE–tabun (B and D; PDB entry 2C0P) with the crystal structures of mAChE·HI-6 (A and B) and mAChE·Ortho-7 (C and D). In the figure, mAChE·HI-6 and mAChE·Ortho-7 are shown in green, TcAChE-VX are shown in blue, mAChE–tabun are shown in cyan and the carbon atoms of the oxime and the phosphorus conjugate are shown in orange and magenta, respectively. The nitrogen atoms are shown in blue, the oxygen atoms are shown in red and the phosphorus atoms are shown in purple. For clarity, residue Asp74, Trp86 and Tyr337 are omitted. (For interpretation of the references to color in this figure legend, the reader is referred to the web version of the article.)

The steric hindrance that Phe338 pose in mAChE–tabun is relevant also for reactivation by Ortho-7 (Fig. 5). Today, obidoxime is considered to be among the most effective reactivators of AChE inhibited by tabun. The ability of Ortho-7 to reactivate AChE inhibited by tabun has not been investigated in detail, but our reactivation experiments indicate that Ortho-7 is superior to HI-6 and slightly better than obidoxime. The ability of Ortho-7 to reactivate tabun conjugates contradicts the suggestion that an oximate in 4-position of the pyridinium ring is necessary to facilitate reactivation of tabun conjugates [32,34]. This controversy can, however, be resolved by the crystal structure of mAChE·Ortho-7 that suggests that the relatively loose binding of the peripheral pyridinium ring and central heptyl linker permit Ortho-7 to evade the steric constraints that Phe338 pose and reactivate even though the oximate is at the 2-position of the pyridinium ring. The structure of mAChE·obidoxime shows a similar, loose binding of the peripheral pyridinium ring, accordingly, obidoxime may be able to circumvent the steric constraints of the tabun conjugate in an analogous fashion.

The pyridinium ring that carries the attacking oxime of Ortho-7 is located in the vicinity of the choline binding site of Trp86 (Fig. 5). In contrast to HI-6, only a slight structural rearrangement of the pyridinium is necessary to position the oximate close to the phosphorus atom. In mAChE·Ortho-7, the oximate oxygen forms a weak hydrogen bond to the main-chain nitrogen of Phe338 (Fig. 5). A rotation of the pyridinium ring from this position towards the phosphorous atom of mAChE-VX and mAChE–tabun places the oximate oxygen at a distance of approximately 2.8–3.0 Å from the phosphorus atom, thus enabling the reactivation to occur after minor rearrangements of the OP-conjugate and the pyridinium ring to achieve an ideal attacking position of the oximate. In the case of obidoxime, a slightly larger rearrangement of the oximate is necessary to obtain a favourable attacking position. Due to the more rigid linker of obidoxime it seems likely that this reorganization also involves the PAS interface. The solvent

exposed PAS interactions of Ortho-7 and obidoxime probably allow these oximes to readily leave the reactivated enzyme.

Apparently, the ability for the oxime to adjust the attacking position in response to different AChE–OP conjugates and their corresponding structural changes of the enzyme is reduced by a short central linker and/or by a highly specific interaction between the PAS and the peripheral pyridinium ring of the oxime. This ability might be important for reactivating certain AChE–OP conjugates such as AChE–tabun that are resistant towards reactivation. On the other hand, the efficiency of HI-6 on reactivating a broad range of hAChE–OP conjugates suggests that a specific interaction with PAS increases the affinity or local concentration of the reactivator and thus promotes reactivation as long as the AChE–OP conjugate does not create steric and/or electrostatic hindrance to the oxime substituted pyridinium ring. Forthcoming studies may provide further experimental support for this hypothesis.

Acknowledgements

We thank Dr. Yngve Cerenius for the assistance at the beam line I711 at the MAX lab synchrotron. The authors also acknowledge Dr. Gertrud Puu, Dr. Andreas Hörnberg and Dr. Anna-Karin Tunemalm for valuable discussions throughout the study.

REFERENCES

[1] Sussman JL, Harel M, Frolow F, Oefner C, Goldman A, Toker L, et al. Atomic structure of acetylcholinesterase from *Torpedo californica*: a prototypic acetylcholine-binding protein. Science 1991;253:872–9.
[2] Barak D, Kronman C, Ordentlich A, Ariel N, Bromberg A, Marcus D, et al. Acetylcholinesterase peripheral anionic site degeneracy conferred by amino acid arrays sharing a common core. J Biol Chem 1994;269:6296–305.
[3] Barak D, Ordentlich A, Bromberg A, Kronman C, Marcus D, Lazar A, et al. Allosteric modulation of acetylcholinesterase activity by peripheral ligands involves a conformational transition of the anionic subsite. Biochemistry 1995;34:15444–52.
[4] Bourne Y, Taylor P, Radic Z, Marchot P. Structural insights into ligand interactions at the acetylcholinesterase peripheral anionic site. Embo J 2003;22:1–12.
[5] Millard CB, Kryger G, Ordentlich A, Greenblatt HM, Harel M, Raves ML, et al. Crystal structures of aged phosphonylated acetylcholinesterase: nerve agent reaction products at the atomic level. Biochemistry 1999;38:7032–9.
[6] Worek F, Reiter G, Eyer P, Szinicz L. Reactivation kinetics of acetylcholinesterase from different species inhibited by highly toxic organophosphates. Arch Toxicol 2002;76:523–9.
[7] Worek F, Thiermann H, Szinicz L, Eyer P. Kinetic analysis of interactions between human acetylcholinesterase, structurally different organophosphorus compounds and oximes. Biochem Pharmacol 2004;68:2237–48.
[8] Wilson IB, Ginsburg S. A powerful reactivator of alkylphosphate-inhibited acetylcholinesterase. Biohem Biophys Acta 1955;18:169–70.
[9] Ginsburg S, Wilson IB. Oximes of the pyridine series. J Am Chem Soc 1957;79:481–5.
[10] Hobbiger F, Sadler PW. Protection by oximes of bis-pyridinium ions against lethal diisopropyl phosphonofluoridate poisoning. Nature 1958;182:1672–3.
[11] Hobbiger F, O'Sullivan DG, Sadler PW. New potent reactivators of acetylcholinesterase inhibited by tetraethyl pyrophosphate. Nature 1958;182:1498–9.
[12] Pang YP, Kollmeyer TM, Hong F, Lee JC, Hammond PI, Haugabouk SP, et al. Rational design of alkylene-linked bis-pyridiniumaldoximes as improved acetylcholinesterase reactivators. Chem Biol 2003;10:491–502.
[13] Hammond PI, Kern C, Hong F, Kollmeyer TM, Pang YP, Brimijoin S. Cholinesterase reactivation in vivo with a novel bis-oxime optimized by computer-aided design. J Pharmacol Exp Ther 2003;307:190–6.
[14] Grosfeld H, Barak D, Ordentlich A, Velan B, Shafferman A. Interactions of oxime reactivators with diethylphosphoryl adducts of human acetylcholinesterase and its mutant derivates. Mol Pharmacol 1996;50:639–49.
[15] Ashani Y, Radic Z, Tsigelny I, Vellom DC, Pickering NA, Quinn DM, et al. Amino acid residues controlling reactivation of organophosphonyl conjugates of acetylcholinesterase by mono- and bisquaternary oximes. J Biol Chem 1995;270:6370–80.
[16] Luo C, Leader H, Radic Z, Maxwell DM, Taylor P, Doctor BP, et al. Two possible orientations of the HI-6 molecule in the reactivation of organophosphate-inhibited acetylcholinesterase. Biochem Pharmacol 2003;66:387–92.
[17] Homstedt B. Synthesis and pharmacology of dimethylamido-ethoxy-phosphoryl cyanide (tabun) together with a description of some allied anticholinesterase compounds containing the N–P bond. Acta Physiol Scand Suppl 1951;90:12–120.
[18] Ekström F, Akfur C, Tunemalm A-K, Lundberg S. Structural changes of phenylalanine 338 and histidine 447 revealed by the crystal structures of tabun-inhibited murine acetylcholinesterase. Biochemistry 2006;45:74–81.
[19] Ellman GL, Courtney KD, Andres Jr V, Feather-Stone RM. A new and rapid colorimetric determination of acetylcholinesterase activity. Biochem Pharmacol 1961;7:88–95.
[20] Kabsch W. Automatic processing of rotation diffraction data from crystals of initially unknown symmetry and cell constants. J Appl Cryst 1993;26:795–800.
[21] Kabsch W. Evaluation of single-crystal X-ray diffraction data from a position-sensitive detector. J Appl Cryst 1988;21:916–24.
[22] Murshudov GN, Vagin AA, Dodson EJ. Refinement of macromolecular structures by the maximum-likelihood method. Acta Crystallogr 1997;D53:240–55.
[23] Brunger AT. Free R value: a novel statistical quantity for assessing the accuracy of crystal structures. Nature 1992;355:472–4.
[24] Jones TA, Zou JY, Cowan SW, Kjeldgaard. Improved methods for building protein models in electron density maps and the location of errors in these models. Acta Crystallogr 1991;A47(Pt 2):110–9.
[25] Laskowski RA, MacArthur MW, Moss DS, Thornton JM. PROCHECK: a program to check the stereochemical quality of protein structures. J Appl Cryst 1993;26:283–91.
[26] Vriend G. WHAT IF: a molecular modelling and drug design program. J Mol Graph Model 1980;8:52–6.
[27] Bourne Y, Kolb HC, Radic Z, Sharpless KB, Taylor P, Marchot P. Freeze-frame inhibitor captures acetylcholinesterase in a unique conformation. Proc Natl Acad Sci USA 2004;101:1449–54.
[28] Hall CR, Inch TD. Phosphorus stereochemistry: mechanistic implications of the observed stereochemistry of bond forming and breaking process at phosphorus in some 5- and 6-membered cyclic phosphorus esters. Tetrahedron 1980;36:2059–95.

[29] Millard CB, Koellner G, Ordentlich A, Shafferman A, Silman I, L. SJ. Reaction products of acetylcholinesterase and VX reveal a mobile histidine in the catalytic triad. J Am Chem Soc 1999;121:9883–4.
[30] Taylor P, Wong L, Radic Z, Tsigelny I, Bruggemann R, Hosea NA, et al. Analysis of cholinesterase inactivation and reactivation by systematic structural modification and enantiomeric selectivity. Chem Biol Interact 1999;119–120: 3–15.
[31] Wong L, Radic Z, Bruggemann RJ, Hosea N, Berman HA, Taylor P. Mechanism of oxime reactivation of acetylcholinesterase analyzed by chirality and mutagenesis. Biochemistry 2000;39:5750–7.
[32] de Jong LP, Verhagen MA, Langenberg JP, Hagedorn I, Loffler M. The bispyridinium-dioxime HLo-7. A potent reactivator for acetylcholinesterase inhibited by the stereoisomers of tabun and soman. Biochem Pharmacol 1989;38:633–40.
[33] Eyer P, Hagedorn I, Klimmek R, Lippstreu P, Loffler M, Oldiges H, et al. HLo 7 dimethanesulfonate, a potent bispyridinium-dioxime against anticholinesterases. Arch Toxicol 1992;66:603–21.
[34] Cabal J, Kuca K, Kassa J. Specification of the structure of oximes able to reactivate tabun-inhibited acetylcholinesterase. Basic Clin Pharmacol Toxicol 2004;95:81–6.